Liver Research 10 (2026) 71–81

Contents lists available at ScienceDirect

Liver Research

journal homepage: http://www.keaipublishing.com/en/journals/liver-research

Original Article

Role of myeloid cell transcription factor EB in alcohol-induced liver injury in mice

Sha Neisha Williams [a], Kafayat Yusuf [b], Xiaojuan Chao [a], Hong-Min Ni [a], Wen-Xing Ding [a,c,*]

[a] Department of Pharmacology, Toxicology and Therapeutics, University of Kansas Medical Center, Kansas City, KS, USA
[b] Department of Surgery, University of Kansas Medical Center, Kansas City, KS, USA
[c] Department of Internal Medicine, University of Kansas Medical Center, Kansas City, KS, USA

ARTICLE INFO

Article history:
Received 3 October 2025
Received in revised form
13 December 2025
Accepted 14 January 2026

Keywords:
Autophagy
Hepatitis
Inflammation
Lysosome
Steatosis
Transcription factor EB (TFEB)

ABSTRACT

Background and aims: Alcohol-associated liver disease (ALD) is a leading cause of liver-related morbidity and mortality worldwide, with no currently effective treatment. ALD is caused by excessive lipid buildup, which eventually triggers inflammation and fibrosis in the liver. Activation of hepatic Kupffer cells (KCs) and macrophages drives liver inflammation, which can worsen alcohol-induced liver injury. The autophagy-lysosome system is crucial for macrophages to support their innate immune functions. Transcription factor EB (TFEB) is a key regulator of autophagy and lysosomal biogenesis, but the role of macrophage TFEB in ALD development is unknown. The aim of this study was to evaluate the effects of Gao-binge alcohol consumption on myeloid cell TFEB and elucidate the role of myeloid TFEB in ALD.
Methods: Two-to-three-month-old male and female LysM Cre^{-} (WT) and LysM Cre^{+} *Tfeb* $^{Flox/Flox\ (f/f)}$ (myeloid-*Tfeb* KO) mice were subjected to chronic alcohol feeding plus an acute binge following the Gao-binge model. Serum alanine aminotransferase, aspartate aminotransferase, triglycerides, and cholesterol content were determined using biochemical assays. Total hepatic protein content and messenger RNA (mRNA) levels of autophagy-related proteins and inflammatory markers were determined using immunoblotting, immunohistochemistry, and real-time quantitative polymerase chain reaction (RT-qPCR). Isolated hepatic infiltrating macrophages and KCs from mice given intragastric ethanol infusions were analyzed by Western blot for TFEB and autophagy-related protein content. Raw 264.7 macrophages were treated with ethanol, lipopolysaccharide (LPS), and LPS plus ethanol to examine nuclear TFEB translocation using immunofluorescence.
Results: We found that TFEB levels were higher in macrophage/KC cells than in hepatocytes and cholangiocytes. While ethanol feeding increased serum alanine aminotransferase and aspartate aminotransferase levels, as well as hepatic triglyceride levels, no significant differences were observed between WT and myeloid-*Tfeb* KO mice. The number of F4/80-positive KCs/macrophages was similar in all four experimental groups, but hepatic neutrophil infiltration increased in alcohol-fed myeloid-*Tfeb* KO mice. LPS or ethanol alone induced nuclear TFEB translocation only moderately in Raw 264.7 macrophages.
Conclusions: Our findings suggest that myeloid TFEB is dispensable for alcohol-induced liver injury in mice.

1. Introduction

The global prevalence rate of alcohol-associated liver disease (ALD) has been steadily increasing in recent years, affecting almost 5% of the global population.[1] Additionally, the National Institute on Alcohol Abuse and Alcoholism (NIAAA) reported in 2022 that

* Corresponding author. Department of Pharmacology, Toxicology and Therapeutics, University of Kansas Medical Center, Kansas City, KS, USA.
E-mail address: wxding@kumc.edu (Wen-Xing Ding).
Peer review under the responsibility of Editorial Office of Liver Research.

https://doi.org/10.1016/j.livres.2026.01.003

alcohol has been associated with more than 46% of liver-related deaths in the United States (The data was collected and compiled by the Centers for Disease Control and Prevention). ALD is considered a spectrum of disorders and pathologies, ranging from increased lipid accumulation to the development of more severe conditions such as alcohol-associated steatohepatitis (ASH) with increased ductular reactions, megamitochondria, inflammation, and fibrosis.[2–4] ALD has been extensively connected to the increased occurrence of liver cirrhosis and hepatocellular carcinoma, labeling it as one of the leading causes of death associated with these debilitating liver diseases.[2,5,6] Toxicity from excessive alcohol consumption leads to the activation of immune cells and increased inflammation in the liver, driven by various pathways that culminate in damage and eventual death of hepatocytes.[7]

A key pathway that is involved in inflammatory signaling and induced by heavy alcohol consumption in the liver is driven by Kupffer cell (KC) activation.[8] In the 1870s, KCs were first identified as the resident macrophages in the sinusoidal space in the liver. These specialized cells are derived from bone marrow precursor cells.[9,10] In the context of alcohol-induced liver injury, KCs respond to inflammatory signaling that is prompted by the generation of highly reactive molecules as well as the direct interaction with bacterial endotoxin, lipopolysaccharide (LPS). Once in the portal circulation, LPS translocates to the liver and binds to a class of receptors termed Toll-like receptors (TLRs) on KCs, inducing their activation. KCs produce inflammatory signaling molecules such as tumor necrosis factor-alpha (TNFα), chemokines, and reactive oxygen species (ROS) that promote further damage to hepatocytes, affecting the overall health of the liver.[8,10,11] Chronic alcohol consumption leads to a continual state of hepatic inflammation, promoting progression from a reversible state to a non-reversible condition of alcohol-induced cirrhosis.[2,12–14]

Similar to its effects on inflammatory signaling, acute and chronic alcohol consumption damages organelles and proteins due to increased amounts of ROS present from alcohol metabolism in the hepatocyte.[15–17] Typically, damaged macromolecules are removed via the degradative process of macroautophagy, also known as autophagy. Autophagy is essential in restoring cellular and metabolic homeostasis in the liver after stress-induced injury and is regulated by several well-established mechanisms.[18–22] One mechanism that regulates autophagy is transcription factor EB (TFEB), a member of the microphthalmia/transcription factor E (MiT/TFE) family. TFEB is most notably known for being a master regulator of autophagy, as it upregulates essential genes involved in both autophagy and lysosomal function.[23–26] TFEB is ubiquitous in its expression across various cell types; however, its activity is higher in cells with high lysosomal activity, such as macrophages.[25,27–30]

Though it has been established that acute alcohol consumption induces autophagy, excessive or chronic alcohol consumption is known to impair this process.[31,32] We have previously shown that hepatic autophagy mediated by TFEB is impaired in alcohol-fed mice using a chronic-on-binge model (Gao-binge model). We showed that alcohol-induced reduction of TFEB led to significant decreases in the expression of lysosomal biogenesis genes, such as lysosomal-associated membrane protein 1 (*Lamp1*) and lysosomal V-ATPases.[31,33] However, the effects of Gao-binge alcohol consumption on myeloid cell TFEB and how myeloid TFEB would affect ALD have yet to be elucidated. In the present study, we established myeloid-specific *Tfeb* knockout mice, and these knockouts and their wild-type counterparts were subjected to chronic alcohol feeding plus an acute binge (Gao-binge) alcohol model. The research aim for this study was to evaluate the role of myeloid TFEB in alcohol-induced liver injury in mice.

2. Materials and methods

2.1. Ethics approval

All procedures were approved by the Institutional Animal Care and Use Committee of the University of Kansas Medical Center (IACUC protocol #: IPROTO2024-387) and were conducted in accordance with international ethical standards. Our study examined both male and female animals, and results are reported for both sexes.

2.2. Animal models

2.2.1. Generation of myeloid cell TFEB KO mice

Tfeb $^{\text{Flox/Flox (f/f)}}$ mice were generated as described previously and were crossed with LysM Cre mice (C57BL/6J) (Jackson Laboratory, Bar Harbor, ME, USA) for six generations.[33] All animals were specific pathogen-free and maintained in a barrier rodent facility under standard experimental conditions.

2.2.2. Gao-Binge alcohol model

Two-to-three-month-old male and female LysM Cre^{-} and LysM Cre^{+} *Tfeb*$^{f/f}$ mice were subjected to the Gao-Binge alcohol model as described previously.[34,35] Briefly, the Lieber-DeCarli liquid control diet (F1259SP, Bio-Serv, Flemington, NJ, USA) was administered to mice for 5 days to allow for acclimation to the diet. On the sixth day, mice were either kept on the control diet or fed the ethanol diet (F1258SP, Bio-Serv, Flemington, NJ, USA; plus 5% ethanol) for 10 days. Post the 10-day feeding period, mice were removed from the liquid diet and given an ethanol gavage (5 g/kg) or a maltose/dextran gavage (9 g/kg; #3653, Bio-Serv, Flemington, NJ, USA). At 8 h post-gavage, mice were anesthetized with Avertin, euthanized, and serum and liver tissues were collected.

Mice were allocated into groups based on sex, genotype, and diet. Male LysM Cre- *Tfeb*$^{f/f}$ mice were divided into control ($n = 7$) and ethanol-fed ($n = 8$) groups, while female LysM Cre- *Tfeb*$^{f/f}$ mice were divided into control ($n = 6$) and ethanol-fed ($n = 8$) groups. Male LysM Cre^{+} *Tfeb* $^{f/f}$ mice comprised control ($n = 7$) and ethanol-fed ($n = 10$) groups, and female LysM Cre^{+} *Tfeb* $^{f/f}$ mice comprised control ($n = 3$) and ethanol-fed ($n = 5$) groups.

2.2.3. Isolation of parenchymal and nonparenchymal cells from mouse liver

Hepatocytes, cholangiocytes, and KCs were isolated from the livers of mice in each experimental group using retrograde, non-recirculating perfusion with 0.05% Collagenase Type IV (#C5138, Sigma-Aldrich, St. Louis, MO, USA) following the protocol as previously described.[36,37] Red blood cells were subsequently removed from the fraction containing cholangiocytes and KCs using Red Blood Cell lysing Buffer (#R7757, Sigma-Aldrich, St. Louis, MO, USA) per manufacturer's instructions. Additionally, both cholangiocytes and KCs were further isolated from the remaining fraction using gradient Percoll (#17-0891-01, GE Healthcare, Chicago, IL, USA) centrifugation as previously described.[36,37]

2.2.4. Fluorescence-activated cell sorting (FACS) isolation for migrating vs. resident hepatic macrophages

C57BL/6J mice were subjected to 6 or 7 weeks of intragastric feeding to develop mouse ASH. Hepatic infiltrating macrophages (IMs) and KCs were isolated as described previously.[38] Briefly, five days after injection of the PKH26-labeled peripheral blood mononuclear cells (PBMCs), IMs (including migrated PBMCs and resident KCs) were isolated from the recipient mice. Isolated cells were incubated with anti-mouse CD16/CD32 for 10 min on ice to block nonspecific binding, and then with the following antibodies:

CD45-V450 (BD Biosciences, Franklin Lakes, NJ, USA), F4/80-FITC (eBioscience, Thermo Fisher Scientific, Waltham, MA, USA), and CX3CR1-APC (R&D Systems, Minneapolis, MN, USA) for 30 min, followed by three washes with cold PBS. For FACS analysis, after gating on $CD45^+$ cells, hepatic macrophages were separated into $PKH26^+$ and $PKH26^-$ groups. IMs are $CD45^+Ly6G^{low}F4/80^{low}CD11b^{high}$, and KCs are $CD45^+Ly6G^{low}$ $F4/80^{high}CD11b^{low}$. Total lysates from IMs and KCs were subjected to Western blot analysis.

2.3. Biochemical assays

To assess liver function and injury, the activities of alanine transaminase (ALT; A7526-625, Pointe Scientific, Canton, MI, USA) and aspartate aminotransferase (AST; A7561-150, Pointe Scientific, Canton, MI, USA) were measured in the serum using commercially available kits, as previously described.[39] Serum and hepatic levels of triglycerides (TGs) and cholesterol were also determined using the corresponding colorimetric kit from Pointe Scientific (TG, #T7532; cholesterol, #C7510; Canton, MI, USA) as previously described.[39]

2.4. Western blot analysis

Total liver and cell lysates were homogenized using radioimmunoprecipitation assay (RIPA) buffer (1% NP40, 0.5% sodium deoxycholate, and 0.1% sodium dodecyl (lauryl) sulfate) supplemented with protease inhibitor cocktail. Protein concentration was measured using the BCA Protein Assay (#23227, Thermo Scientific, Rockford, IL, USA). Liver lysates were loaded at 30 μg and cell lysates were loaded at 3 μg of protein for electrophoretic separation on a 12% sodium dodecyl sulfate-polyacrylamide gel electrophoresis (SDS-PAGE) gel and transferred to a polyvinylidene fluoride (PVDF) membrane. Membranes were then blocked for 1 h at room temperature in 5% blocking solution containing evaporated milk and Tris-buffered Saline plus 0.1% Tween-20 (TBST) and probed with the appropriate primary antibodies overnight at 4 °C, followed by incubation with secondary antibodies for 1 h on the next day. Antibodies used for Western blot are listed in Table 1. After incubation with secondary antibodies, membranes were washed three times in TBST in 5-min intervals. SuperSignal West Pico Plus chemiluminescent substrate (#34578, Thermo Scientific, Rockford, IL, USA) was used to develop the membranes for protein visualization. The membranes were imaged using the Li-Cor Odyssey Fc imaging system and densitometry analysis was performed with ImageJ software (NIH).

2.5. Histology and immunohistochemistry

Paraffin-embedded liver sections (5 μm thick) were stained using hematoxylin and eosin (H&E) for visualization of liver histology. For immunohistochemistry, liver sections were deparaffinized, followed by 3% hydrogen peroxide treatment for quenching. Tissue sections were treated with citrate buffer pH 6.0 for heat-induced antigen retrieval. After antigen retrieval, liver sections were blocked using UltraVision Protein Block (Epredia, TA-125-PBQ, Kalamazoo, MI, USA) to prevent non-specific background staining. Post-blocking, slides were incubated with primary antibody overnight at 4 °C and with the appropriate secondary antibody at 37 °C for 1 h the next day. Antibodies used for immunohistochemistry are listed in Table 1. Positive staining was developed using ImmPACT NovaRED HRP substrate (Vector Laboratories, SK-4805, Newark, CA, USA) and counterstained with hematoxylin for nuclear staining. Tissue sections were visualized at 20 × for positively stained areas using microscopy.

2.6. Cell culture and immunofluorescence staining

Raw 264.7, macrophage cells, a mouse monocyte/macrophage cell line from ATCC, were used. Cells were thawed and plated in a 100 mm dish and maintained with Dulbecco's Modified Eagle medium (DMEM) high glucose cell culture medium (Gibco, Thermo Fisher Scientific, 11965092, Rockford, IL, USA) supplemented with 10% fetal bovine serum (FBS), 1% penicillin/streptomycin as the antibiotic, and 1% L-glutamine. Raw 264.7 macrophage cells were grown on coverslips placed in a 12-well plate. Cells were allowed to adhere overnight and treated with the following chemicals: 250 nmol/L Torin1, 100 ng/mL LPS, 80 mmol/L ethanol (EtOH), or a combination of 100 ng/mL LPS and 80 mmol/L (mM) EtOH. Cells treated with Torin1 or LPS were incubated for 2 h, whereas those treated with EtOH were incubated for 6 h. After the incubation period, cells were washed with 1× phosphate-buffered saline (PBS) and then fixed in 4% paraformaldehyde (PFA in PBS) at 4 °C overnight. After fixation, coverslips were washed with 1× PBS and blocked in blocking buffer

Table 1
List of antibodies used for Western blots, immunohistochemistry, and immunofluorescence.

Antibody	Source	Cat#
β-actin	Sigma-Aldrich	A5441
CK19	Developmental Studies Hybridoma Bank (University of Iowa, Iowa City, USA)	TROMA-III
F4/80 monoclonal antibody (BM8)	Thermo Fisher Scientific	14-4801
GAPDH	Cell Signaling Technology	2118
HNF4α (P1/P2)	Perseus Proteomics	PP-H1415-00
LAMP-2	Developmental Studies Hybridoma Bank	ABL-93-c
LC3	Made by the lab, available by request	N/A
Ly-6G	Cell Signaling Technology	87048S
p62	Abnova	H00008878-M01
TFEB	Thermo Fisher Scientific	A303-673A
VATPv1A	Proteintech	17115-1-AP
VATPv1B2	Proteintech	15097-1-AP
HRP-Goat Anti-Mouse IgG	Jackson ImmunoResearch	115-035-146
HRP-Goat Anti-Rabbit IgG	Jackson ImmunoResearch	111-035-144
HRP-Goat Anti-Rat IgG	Jackson ImmunoResearch	112-035-143
Alexa Fluor® 488 AffiniPure® Goat Anti-Rabbit IgG	Jackson ImmunoResearch	111-545-144
Alexa Fluor® 594 AffiniPure® Goat Anti-Mouse IgG	Jackson ImmunoResearch	115-585-003
Rhodamine Red™-X AffiniPure® Goat Anti-Rat IgG	Jackson ImmunoResearch	112-295-167
HRP Horse Anti-Rabbit IgG	Vector Laboratories	MP-7401
HRP Goat Anti-Rat IgG	Vector Laboratories	MP-7444-15

(1× PBS, 0.4% Triton X-100, and 10% goat serum) for 1 h at room temperature. Next, cells were incubated in the appropriate primary antibodies (diluted in staining buffer containing 1× PBS, 0.4% Triton X-100, and 2% goat serum) overnight at 4 °C. Cells were then washed in 1× PBS, followed by incubation in secondary antibodies (diluted in the above-mentioned staining buffer) for 1.5 h at room temperature. The coverslips were washed with 1× PBS to remove the secondary antibody solution. Antibodies used for immunofluorescence are listed in Table 1. The cover slips were incubated with Hoechst 33342 (Thermo Fisher Scientific, Waltham, MA, USA) for nuclear staining for 10 min at room temperature, then washed with 1× PBS and mounted to microscope slides. Cells were imaged using a Nikon fluorescence microscope (Melville, NY, USA).

2.7. RNA isolation from liver tissue and reverse transcription

Frozen liver tissue from each treatment group was homogenized and used for isolating RNA following the protocol for TRIzol Reagent (#15596018, Invitrogen, Carlsbad, CA, USA). Briefly, samples were mixed with chloroform and centrifuged. After centrifugation, the aqueous form was removed and used for RNA precipitation. Samples were then mixed with 100% isopropanol for the precipitation step, followed by 12000 *g* for 10 min. Lastly, the pellet was washed in 75% ethanol, centrifuged at 7500 *g* for 5 min, and resuspended in RNase-free water.

Purified RNA for both cells and liver tissue was used to synthesize first-strand cDNA using reverse transcription according to the Maxima H Minus First Strand cDNA synthesis kit protocol (Thermo Fisher Scientific, K1652, Rockford, IL, USA). Briefly, template RNA (3 μg) was mixed with Oligo(dT)18, dNTP mix, 5× RT buffer, RiboLock RNase inhibitor, Maxima H Minus reverse transcriptase, and nuclease-free water, and then amplified using a thermocycler to generate complementary DNA (cDNA).

2.8. RT-qPCR

Real-time quantitative polymerase chain reaction (RT-qPCR) was used to determine the mRNA expression levels of select genes using a Bio-Rad CFX384 real-time PCR detection system and SYBR Green mix (#B21202, Biomake, Bio-Connect, Netherlands). *Actin* or *18s* was used as the housekeeping gene for normalization. The mRNA expression of the following genes was determined: *Tnfα, Il-1b, Ly6g, Adgre1, Mcp-1, Mip-1α, Mip-2,* and *Cxcl-1*. The fold change for each gene was expressed relative to the control diet-fed LysM Cre^{-}*Tfeb*$^{f/f}$ mice (Table 2). Calculation of the fold change for each gene was performed using the $^{\Delta\Delta}$Ct method.

Table 2
Sequences of primers for quantitative real-time PCR analysis.

Gene	Forward primer (5'-3')	Reverse primer (5'-3')
Actin	TGTTACCAACTGGGACGACA	GGGGTGTTGAAGGTCTCAAA
18s	GAGCGAAAGCATTTGCCAAG	GGCATCGTTTATGGTCGGAA
Tnfα	CGTCAGCCGATTTGCTATCT	CGGACTCCGCAAAGTCTAAG
Ly6g	TGCGTTGCTCTGGAGATAGA	CAGAGTAGTGGGGCAGATGG
Il-1b	GCCCATCCTCTGTGACTCAT	AGGCCACAGGTATTTTGTCG
Adgre1	CTTTGGCTATGGGCTTCCAGTC	GCAAGGAGGACAGAGTTTATCGTG
Mcp-1	CCAGCCTACTCATTGGGAT	GGGCCTGCTGTTCACAGTT
Mip-1α	TGAGAGTCTTGGAGGCAGCGA	TGTGGCTACTTGGCAGCAAACA
Mip-2	CTCAGAGGAAGACGATGAAG	GACGAGTTATCCCAGCCAAA
Cxcl-1	GCTGGGATTCACCTCAAGAA	CTTGGGGACACCTTTTAGCA

Abbreviations: Adgre1, adhesion G-protein-coupled receptor E1; CXCL-1, C-X-C motif chemokine ligand 1; IL-1b, interleukin-1 beta; MCP-1, monocyte chemoattractant protein-1; MIP-1α, macrophage inflammatory protein-1alpha; MIP-2, macrophage inflammatory protein-2; TNFα, tumor necrosis factor-alpha.

2.9. Statistical analysis

Statistical analysis was performed using GraphPad Prism software (version 9.4.1 (681), GraphPad Software, Boston, MA, USA). All experimental data were expressed as mean ± standard error of the mean (SEM). Either one-way analysis of variance (ANOVA) followed by Tukey's post-hoc test or two-tailed Student's *t*-test was used where appropriate. A *P* value less than 0.05 was considered significant.

3. Results

3.1. Expression of TFEB is much higher in KCs than in hepatocytes and cholangiocytes in the mouse liver

To determine the expression levels of TFEB in different cell types in the mouse liver, hepatocytes, cholangiocytes, and KCs were isolated, and an equal amount of cellular lysates was subjected to Western blot analysis. As can be seen in Fig. 1A, the levels of TFEB were much higher in KCs followed by hepatocytes, with no detectable levels in cholangiocytes. Immunofluorescence staining with an F4/80 antibody confirmed that the isolated KCs were F4/80 positive (Fig. 1B). The levels of TFEB in KCs isolated from LysM Cre^{+} (myeloid-*Tfeb* KO) mouse livers were significantly lower than those in KCs from LysM Cre^{-} (WT) mouse livers using Western blot analysis (Fig. 1C) and immunofluorescence staining (Fig. 1D), confirming the successful deletion of *Tfeb* in myeloid-*Tfeb* KO mice. The levels of LC3-II were also much lower in KC isolated from myeloid-*Tfeb* KO mice than in WT mice, likely due to impaired autophagy in KCs as a result of TFEB deletion. Analysis of the published human single-cell RNA-seq dataset (GSE255772) showed that TFEB is highly expressed in monocytes/macrophages and neutrophils,[40] but relatively low in hepatocytes (Fig. 1E). Additionally, KCs and IMs were isolated from the livers of mice administered intragastric ethanol infusions for 6 or 7 weeks to evaluate differences in the expression of several lysosomal proteins. The protein levels of TFEB-targeted genes, including LAMP2, VATPv1a, and VATPv1b2, were higher in KCs but barely detectable in IMs. Additionally, seven weeks of alcohol feeding further increased the levels of these lysosomal proteins in KCs (Fig. 1F). Overall, these data suggest that TFEB is primarily expressed in immune cells rather than hepatocytes in mouse livers.

3.2. Loss of myeloid cell TFEB did not worsen Gao-binge alcohol-induced liver injury

The levels of serum ALT were increased approximately 2-fold and 7-fold in Gao-binge alcohol-fed male ($P < 0.05$) and female WT mice, respectively, compared with control diet-fed WT mice (Fig. 2A). There was an appreciable 2-fold increase in AST levels in alcohol-fed female WT mice, though not significant (Fig. 2B). The levels of serum ALT and AST in Gao-binge alcohol-fed female myeloid-*Tfeb* KO mice were similar to those in Gao-binge alcohol-fed female WT mice (Fig. 2A and B). There were no significant changes in liver-to-body weight ratios among all the groups (Fig. 2C). Gao-binge alcohol feeding significantly raised ($P < 0.05$) serum alcohol levels to similar concentrations across genotypes in both male and female mice (Fig. 2D). Gao-binge alcohol feeding also increased hepatic TG levels, but no differences were observed between WT and myeloid-*Tfeb* KO mice. The hepatic TG levels in Gao-binge alcohol-fed female mice tended to be higher than in males, regardless of genotype, although these differences did not reach statistical significance (Fig. 2E). Consistent with the hepatic TG data, H&E staining showed an increased number of lipid

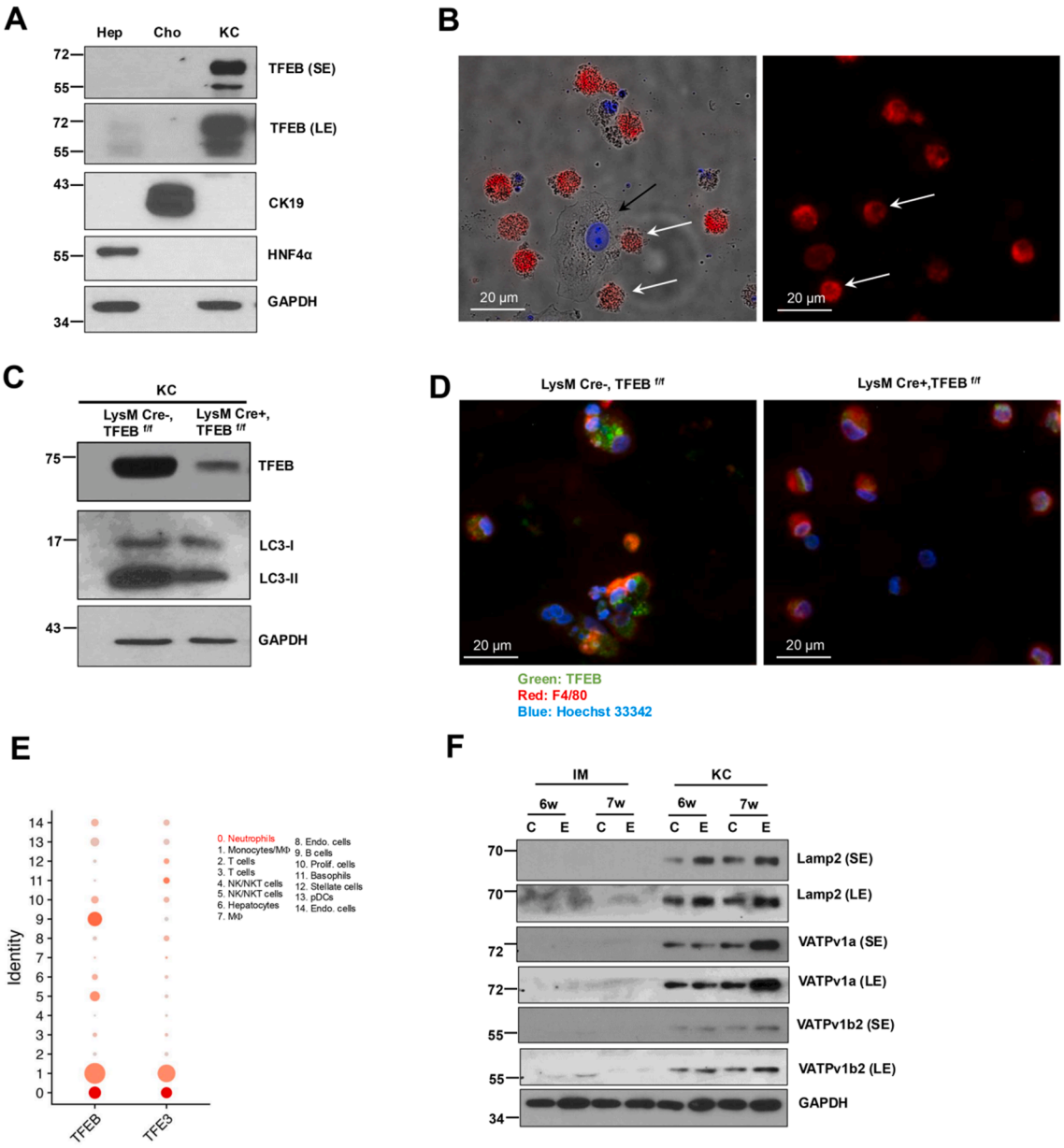

Fig. 1. TFEB is highly expressed in mouse Kupffer cells/macrophages but not hepatocytes and cholangiocytes. Primary hepatocytes (Hep), cholangiocytes (Cho), and Kupffer cells (KCs) were isolated from wild-type mice, and total cell lysates of these cells were subjected to Western blot analysis **(A)**. **(B)** Isolated KCs from WT mice were immuno-stained for F4/80. Hoechst 33342 was used to stain the nuclei, followed by fluorescence microscopy and phase-contrast imaging. White arrows denote F4/80 positive KCs, and the black arrow denotes a hepatocyte. **(C)** KCs were isolated from LysM Cre^{-} (WT) and LysM Cre^{+} *Tfeb* $^{f/f}$ (myeloid-*Tfeb* KO) mice, and total lysates were used for Western blot analysis. **(D)** KCs were isolated from WT and myeloid-*Tfeb* KO mice and were immuno-stained for TFEB and F4/80. Hoechst 33342 was used to stain the nuclei, followed by fluorescence microscopy. Representative images are shown. **(E)** Bioinformatic analysis of single-cell RNAseq for TFEB and TFE3 expression in human livers of a published public dataset (GSE255772). **(F)** C57BL/6J mice were subjected to intragastric alcohol feeding for 6 and 7 weeks. IMs and KCs were isolated, and total cell lysates were used for Western blot analysis. Molecular mass markers are indicated in kDa. Abbreviations: C, control; CK19, cytokeratin 19; E, ethanol; SE, short exposure; LE, long exposure; HNF4α, hepatocyte nuclear factor 4-alpha; IMs, infiltrating macrophages; NKT cells, natural killer T cells.

droplets in Gao-binge alcohol-fed both WT and KO mice (Fig. 2F arrows). Together, these data indicate that myeloid TFEB is dispensable for Gao-binge alcohol-induced liver injury and steatosis.

3.3. Loss of TFEB in KCs results in increased hepatic neutrophils and decreased cytokine production in myeloid-Tfeb KO mice exposed to Gao-binge alcohol

Staining for the macrophage surface marker, F4/80, did not reveal any significant changes between the control diet and ethanol diet-fed groups of both WT and myeloid-*Tfeb* KO mice (Fig. 3A and B). Additionally, neutrophil accumulation was determined using the neutrophil surface marker, Ly6G. As shown in Fig. 3A and C, IHC staining of Ly6G in control diet and Gao-binge alcohol-fed WT mice showed no significant differences, whereas the number of Ly6G-positive neutrophils was the highest in Gao-binge alcohol-fed myeloid-*Tfeb* KO mice compared to all other groups. This increased trend in Ly6G levels in myeloid-*Tfeb* KO mice was further observed quantitatively using RT-qPCR (Fig. 3D). Interestingly, hepatic mRNA levels of several other inflammatory genes were either unchanged (such

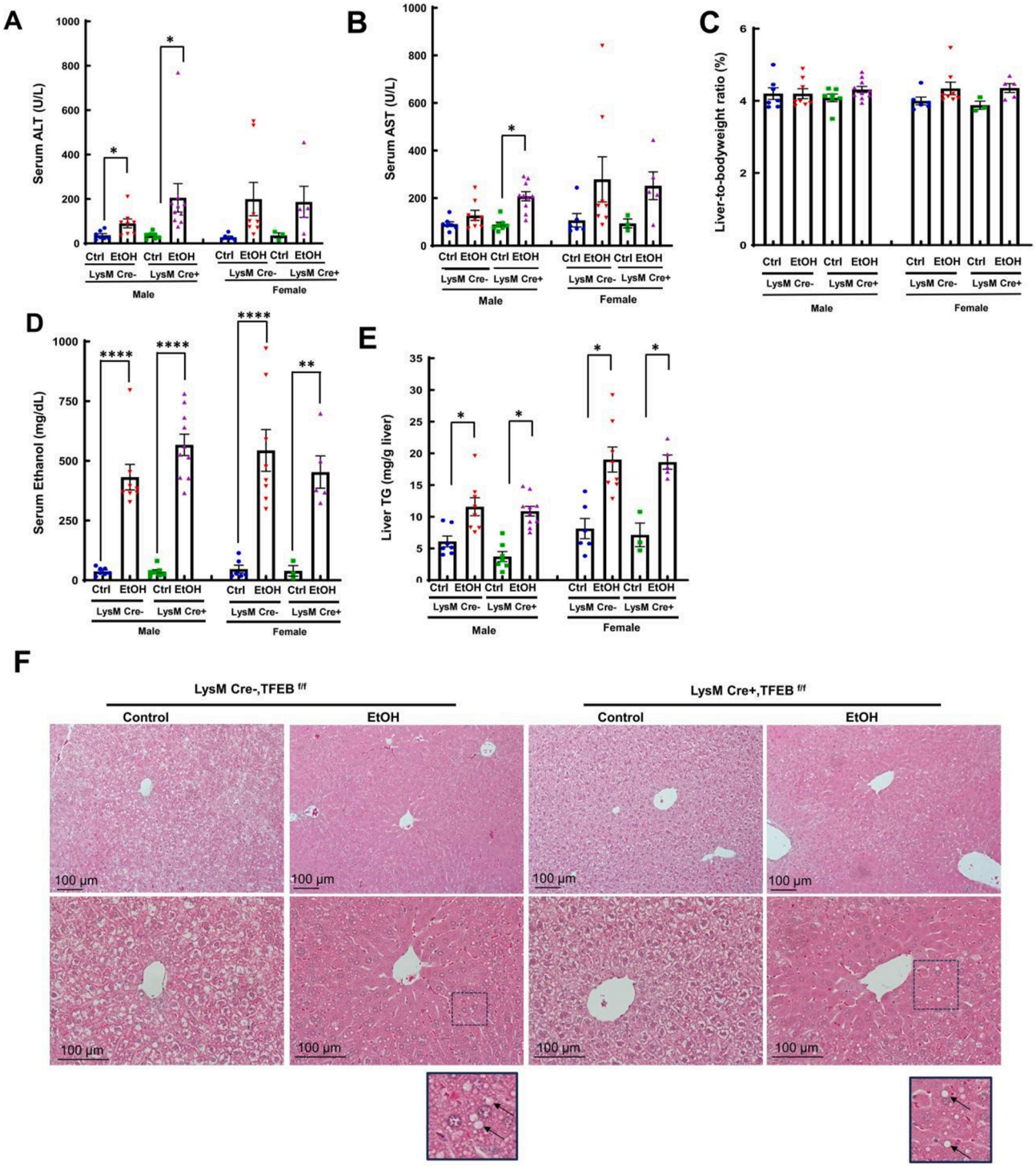

Fig. 2. Loss of myeloid TFEB did not exacerbate Gao-binge alcohol-induced hepatic steatosis and liver injury. Female and male two-to-three-month-old LysM Cre^{-} (WT) and LysM Cre^{+} *Tfeb* $^{f/f}$ (myeloid-*Tfeb* KO) mice were subjected to the Gao-binge alcohol feeding. **(A–B)** Serum ALT and AST levels were measured. **(C)** Liver-to-body weight ratios were determined. **(D)** Serum ethanol concentrations and **(E)** hepatic TGs were measured. Data are presented as mean ± SEM (n = 3–10). **(F)** Representative images of H&E staining of liver tissues from male control diet and alcohol diet-fed WT and myeloid-*Tfeb* KO mice are shown. Lower panel images were enlarged graphs from the boxed areas, indicating lipid droplets in hepatocytes (arrows). $^{*}P < 0.05$, $^{**}P < 0.01$, $^{****}P < 0.0001$. Abbreviations: ALT, alanine aminotransferase; AST, aspartate aminotransferase; Ctrl, control diet; EtOH, ethanol diet; TGs, triglycerides.

as *Mcp-1* and *Adgre1*) or decreased (*Il-1b, Cxcl1*, and *Tnfα)* in Gao-binge alcohol-fed WT and myeloid-*Tfeb* KO mice compared to control diet-fed WT mice (Fig. 3D). Taken together, these results suggest that myeloid-TFEB may play a role in modulating hepatic neutrophil infiltration but not macrophages and expression of hepatic cytokines/chemokines.

3.4. Alcohol consumption leads to insufficient autophagy in LysM Cre^{+} Tfeb$^{f/f}$ mice

Compared to the control diet-fed mice, hepatic levels of TFEB protein were markedly decreased in Gao-binge alcohol fed WT mice. Quantitative analysis showed an increased trend in the levels

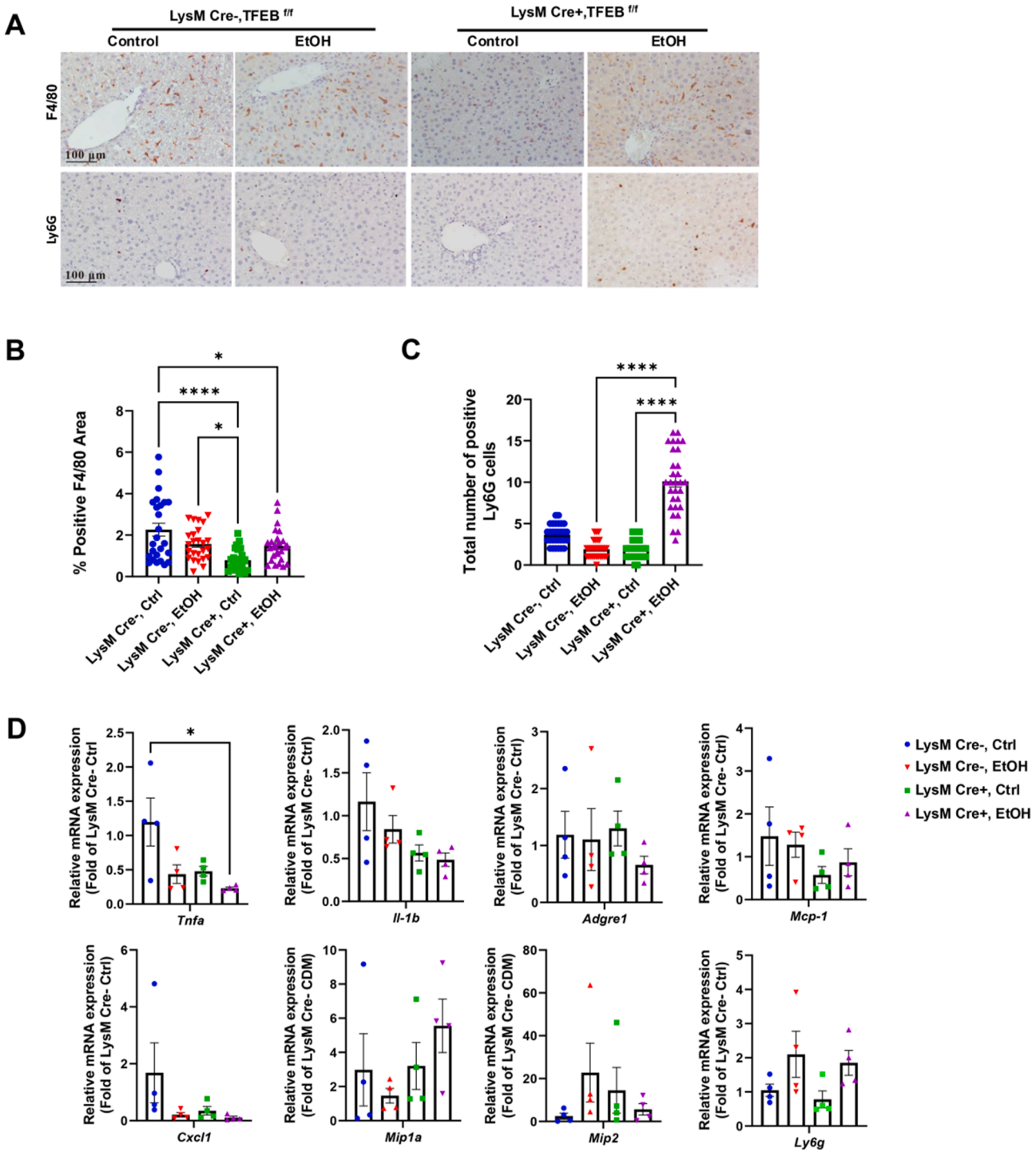

Fig. 3. Increased hepatic neutrophil infiltration in Gao-binge alcohol fed LysM Cre^{+}*Tfeb* $^{f/f}$ mice. Male 6–8 weeks old LysM Cre^{-} (WT) and LysM Cre^{+}*Tfeb* $^{f/f}$ (myeloid-*Tfeb* KO) mice were subjected to the Gao-binge alcohol feeding. **(A)** Representative images of immunohistochemistry staining for hepatic F4/80 and Ly6G. **(B–C)** Quantitative analysis of liver F4/80 and Ly6G staining (8–10 images per mouse, $n = 3$). **(D)** qRT-PCR results for the mRNA expression of the following inflammatory markers: *Tnfα, Il-1b, Adgre1, Mcp-1, Cxcl1, Mip1a, Mip2,* and *Ly6g*. $^{*}P < 0.05$, $^{****}P < 0.0001$. Abbreviations: Ctrl, control diet; EtOH, ethanol diet.

of LC3-II with decreased p62, confirming insufficient hepatic autophagy as we previously reported.[31] Gao-binge alcohol feeding did not alter the levels of TFEB and p62 but increased hepatic LC3-II ($P < 0.05$) (2.5-fold increase over control-diet fed WT mice) in myeloid-*Tfeb* KO mice (Fig. 4), likely due to further impaired autophagy. These results further suggest that alcohol impairs hepatic autophagy in WT mice, which may be worsened in myeloid-*Tfeb* KO mice.

3.5. Ethanol and LPS moderately increase nuclear translocation of TFEB in RAW macrophages

To investigate the localization of myeloid cell TFEB in macrophages under stress-induced conditions, Raw 264.7 macrophage cells were treated with various stressors such as LPS, EtOH, and a combination of both LPS and EtOH. As a positive control, cells were also treated with Torin1, as it is known to stimulate TFEB nuclear

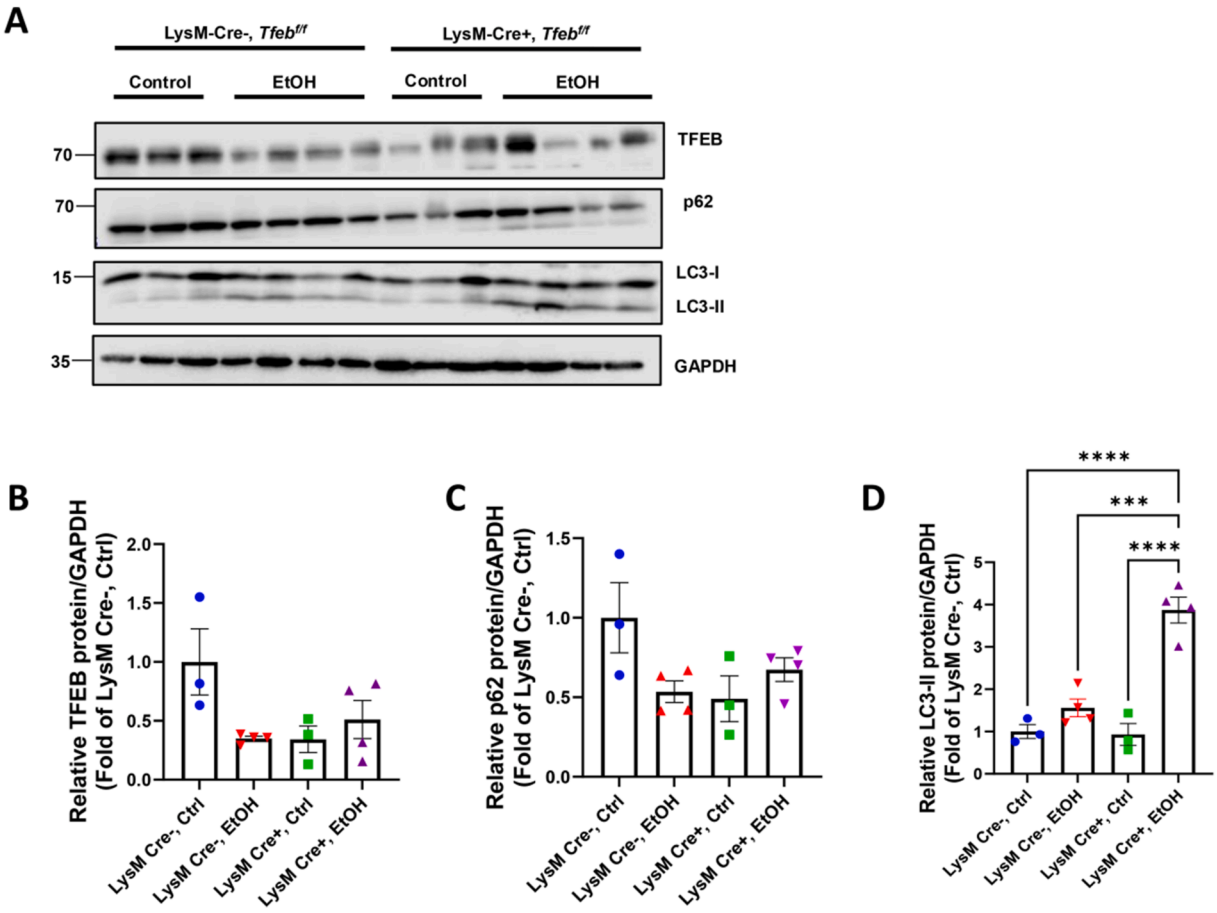

Fig. 4. Gao-binge alcohol induces insufficient hepatic autophagy in myeloid-*Tfeb* KO mice. Male 6–8 weeks old LysM Cre^{-} (WT) and LysM Cre^{+} *Tfeb* $^{f/f}$ (myeloid-*Tfeb* KO) mice were subjected to the Gao-binge alcohol feeding. **(A)** Total liver lysates were subjected to Western blot analysis for proteins associated with autophagy. **(B–D)** Densitometry analysis of **(A)**. Data are presented as means ± SEM ($n = 3$–4). $^{***}P < 0.001$, $^{****}P < 0.0001$. Molecular mass markers are indicated in kDa. Abbreviations: Ctrl, control diet; EtOH, ethanol diet.

translocation by preventing the mechanistic target of rapamycin complex 1 (mTORC1)-mediated inhibitory phosphorylation of TFEB.[41] Torin1-treated macrophages had a significant increase ($P < 0.05$) in nuclear TFEB translocation in Raw 264.7 macrophages. EtOH or LPS treatment alone or the combination of EtOH and LPS only led to a moderate increase in nuclear TFEB translocation in macrophages (Fig. 5A and B). Together, these results suggest that LPS and EtOH moderately increase nuclear TFEB translocation in cultured macrophages.

4. Discussion

Though the function of hepatic TFEB in the context of alcohol-induced liver injury has been previously studied,[31,33] the role and mechanisms by which myeloid cell TFEB contributes to alcohol-induced liver injury have not been studied. Acute and chronic alcohol consumption induces the production of the harmful metabolites acetaldehyde and ROS and can disrupt the barrier between enterocytes, promoting the release of LPS into the enterohepatic portal circulation.[8,11,12] These events trigger KC and macrophage activation and increase the expression of various genes involved in inflammatory, chemoattractant, and antimicrobial responses associated with the activation of several transcription factors, including nuclear factor kappa B (NF-κB), the interferon-regulatory factor (IRF) family proteins, and cAMP-response element binding protein 1 (CREB1).[42] In response to pathogen exposure, the autophagy-lysosome system plays critical roles in macrophages to promote antigen processing and presentation, degradation of phagocytosed pathogens, secretion of NK and T-cell cytotoxic granules, and TLR signaling.[43] Additionally, autophagy in macrophages can help engulf intracellular pathogens and modulate inflammatory signaling through the inflammasome complex.[44] Furthermore, macrophage TFEB is associated with the production and secretion of inflammatory mediators such as C–C motif chemokine ligand 2, IL-1β, and colony-stimulating factor-1.[45] Indeed, alcohol fed myeloid-specific *Atg5* KO mice had increased proinflammatory cytokine gene induction and hepatocyte death without affecting hepatic steatosis compared with alcohol-fed wild-type mice, highlighting a protective role of macrophage autophagy in protecting against ALD via anti-inflammatory effects.[46] In contrast to myeloid-specific *Atg5* KO mice, our study found that the myeloid-specific deletion of *Tfeb* in mice does not affect liver injury or increase the expression of inflammatory cytokines and chemokines.

Several reasons may explain the different observations in myeloid-specific *Atg5* KO and *Tfeb* KO mice after alcohol exposure. Myeloid-specific *Atg5* KO mice were fed 5% ethanol for 21 days, with a final ethanol gavage and LPS injection on the last day before euthanasia. In contrast, myeloid-*Tfeb* KO mice underwent the Gao-binge alcohol model, which involved 10 days of 5% ethanol feeding and a single ethanol gavage without LPS. ATG5 is an essential autophagy protein that complexes with ATG-12 and ATG16L for

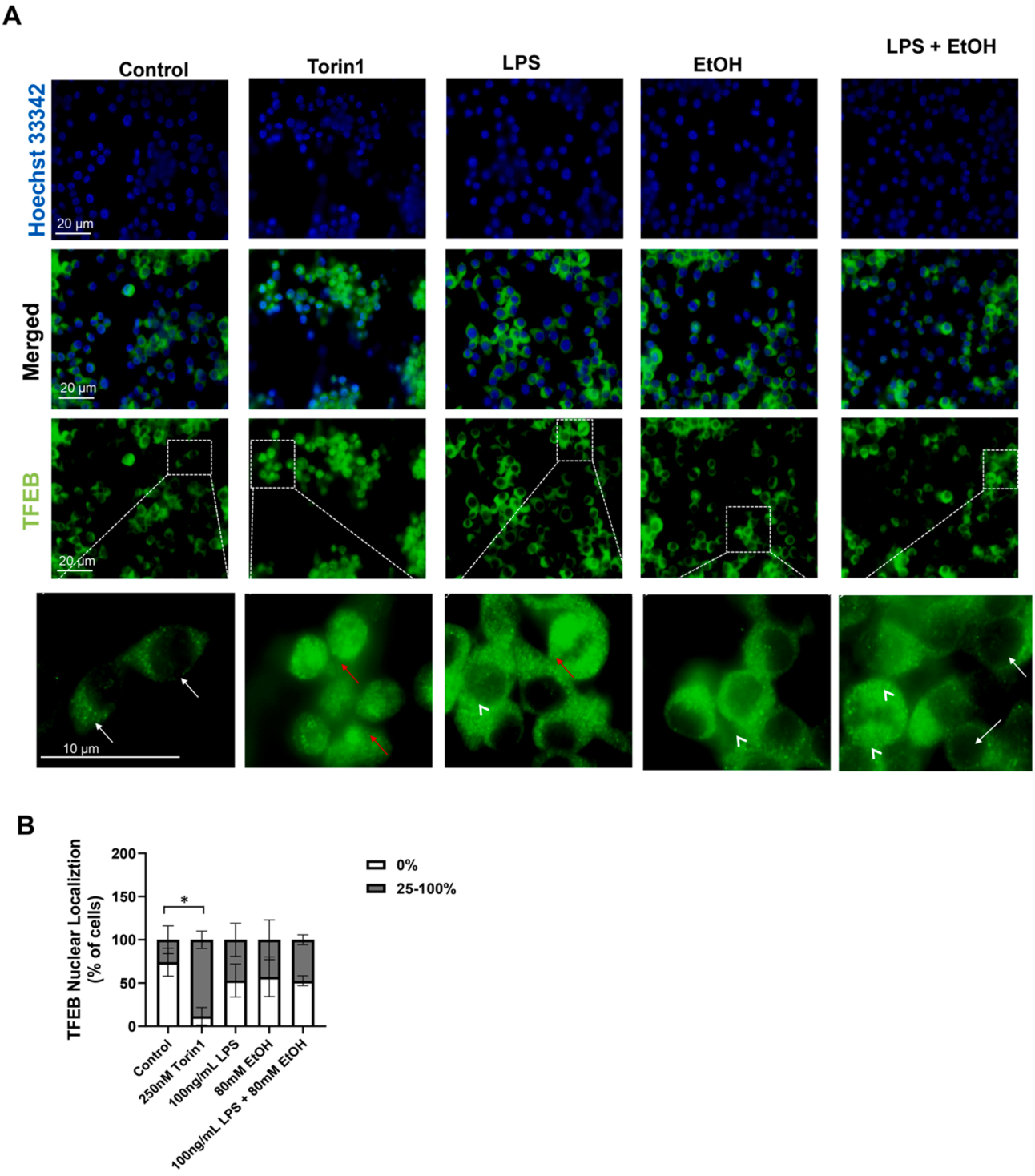

Fig. 5. LPS and EtOH treatment moderately increase nuclear TFEB translocation in Raw 264.7 macrophages. Mouse Raw 264.7 macrophages were plated and treated with the following compounds: 250 nmol/L Torin1 for 2 h, 100 ng/mL lipopolysaccharide (LPS) for 2 h, 80 mmol/L (mM) ethanol (EtOH) for 6 h, or the combination of 100 ng/mL LPS (2 h) and 80 mmol/L (mM) EtOH (6 h). Cells were fixed followed by immunofluorescence staining and fluorescence microscopy. Hoechst 33342 was used to stain the cell nuclei. **(A)** Representative immunofluorescent images are shown, taken at 60× magnification. **(B)** Quantification of the ratio of TFEB nuclear-to-cytoplasmic localization. The lower panels are enlarged graphs from the boxed areas. White arrows denote cytosolic TFEB, red arrows denote nuclear TFEB, and arrowheads denote both cytosolic and nuclear TFEB. Hoechst 33342 was used as a nuclear stain. 117–199 cells were counted per treatment. Data are shown as means ± SEM ($n = 3$). $^{*}P < 0.05$.

autophagosome formation. Deletion of ATG5 in the mouse liver severely impairs hepatic autophagy, whereas deletion of hepatic *Tfeb* in mice shows no phenotypes. Unlike ATG5, TFEB belongs to the microphthalmia-associated transcription factor (MiTF) family of proteins, which also includes MiTF, TFE3, and TFEC in mammalian cells.[24] It is well known that these transcription factors all bind to the Coordinated Lysosomal Expression and Regulation (CLEAR) sequence and have overlapping functions, so the loss of one can be compensated by the others.[47] Indeed, mice with deletion of TFEB alone in the liver or pancreas show no obvious

effects, but double deletion of TFEB and TFE3 made mice more susceptible to pancreatitis and alcohol-associated hepatitis.[33,48,49] Therefore, the absence of noticeable increased liver injury in myeloid- *Tfeb* KO mice compared with WT mice after Gao-binge alcohol may be due to the compensatory effects of other MiTF family proteins in macrophages. Future studies should involve deleting TFE3 or TFEC in myeloid- *Tfeb* KO mice to better understand the role of MiTF family transcription factors in lysosomal biogenesis during ALD.

In addition to its role in the activation of KCs and other macrophages, chronic alcohol exposure has been documented to trigger F4/80^{+} KC death through the induction of apoptosis, resulting in as much as a 10% reduction in KC population in some studies.[50,51] Additionally, this apoptosis was found to be driven by factors such as alcohol-induced phosphorylation of FOXO3 as well as the increased production of growth differentiation factor 15 (GDF15) derived from elevated catecholamine levels in the liver.[50,52] A loss of KC population has been reported to be restored by circulating monocytes recruited to sites of inflammation in the liver induced by chronic ethanol exposure. Eventually, these monocytes will differentiate into an anti-inflammatory phenotype to mitigate proinflammatory signaling, an observation made in both human alcohol-associated hepatitis (AH) and animal models.[50,53,54] Increased circulation and hepatic infiltration of neutrophils have been observed in human AH patients as well. Elevated neutrophil levels are generally believed to be harmful in the development of ALD, but recent single-cell studies have shown that neutrophils are highly diverse, explaining their varied roles in ALD progression. For example, recent studies identified a subset of interleukin-8 (IL-8) positive neutrophils as key drivers of severe AH progression.[40,55] Hepatic neutrophil infiltration is guided by various chemokines such as C-X-C motif chemokine ligand 1 (CXCL1), MIP-2, and IL-8. We found that Gao-binge alcohol feeding reduced hepatic *Cxcl1* expression, which was already lower even in control diet-fed myeloid-*Tfeb* KO mice. Interestingly, the number of hepatic neutrophils was significantly higher ($P < 0.05$) in alcohol-fed myeloid-*Tfeb* KO mice in comparison to WT control and Gao-binge fed as well as myeloid-*Tfeb* KO control diet-fed mice. The observed reduction in hepatic *Cxcl1* expression in alcohol-fed *Tfeb* KO mice might indicate a secondary feedback inhibition caused by increased neutrophil infiltration. Measuring hepatic and circulating levels of CXCL1 in these mice would provide more insights to better understand these findings. Nonetheless, it appears that the absence of myeloid-specific TFEB may promote hepatic neutrophil infiltration.

Our study also offered some insights on whether ethanol or LPS would affect TFEB nuclear translocation in macrophages. It has been well documented that TFEB nuclear translocation is regulated mainly via its phosphorylation by mTORC1. mTORC1-mediated phosphorylation of TFEB results in its cytosolic retention and degradation. Indeed, we found that inhibition of mTORC1 by Torin 1 increased nuclear TFEB translocation in Raw 264.7 macrophages. Interestingly, LPS or ethanol alone only moderately increased TFEB nuclear translocation in the macrophages, and the combination of both ethanol and LPS did not further increase nuclear TFEB translocation. As ethanol is metabolized into acetaldehyde mainly in hepatocytes by alcohol dehydrogenase and acetaldehyde dehydrogenase, future studies are needed to investigate whether acetaldehyde would affect TFEB nuclear translocation in macrophages.

Although this study provided some insight into the role of myeloid TFEB in ALD models, several limitations remained. First, alcohol-induced changes to autophagy-related proteins and inflammatory signaling were only investigated in whole liver lysates from myeloid-*Tfeb* KO mice and their wild-type counterparts. Flow cytometry analysis of macrophage and neutrophil polarization in isolated macrophages and neutrophils from myeloid-*Tfeb* KO and WT mice would provide further insight into the roles of TFEB and chronic alcohol exposure in the overall functionality of these myeloid cells. As previously discussed, TFEB belongs to the MiTF family of transcription factors that includes TFEB analogs of TFE3, MiTF, and TFEC. It is highly likely that other MiTF members may compensate for the loss of TFEB. Deletion of either TFE3 or TFEC in conjunction with TFEB in myeloid cells would provide additional insight into the roles of myeloid cell autophagy and inflammatory signaling in ALD. In addition, we only measured the mRNA changes of the chemokines, which may not necessarily reflect the protein changes of these chemokines. Future studies are needed to measure protein changes and further clarify the role of myeloid TFEB-mediated inflammatory response in ALD. Macrophage lysosomes are critical for clearing neutrophils, especially apoptotic neutrophils by efferocytosis. Future studies are needed to determine whether the loss of TFEB in macrophages may affect the clearance of neutrophils, resulting in prolonged neutrophil retention.

5. Conclusions

This study demonstrated that the loss of myeloid TFEB is not necessary for alcohol-induced liver injury. Although neutrophil infiltration increased in livers lacking myeloid TFEB, liver injury was not further worsened.

Authors' contributions

Sha Neisha Williams: Writing – original draft, Validation, Investigation, Formal analysis, Data curation. **Kafayat Yusuf:** Investigation, Formal analysis, Data curation. **Xiaojuan Chao:** Formal analysis, Data curation. **Hong-Min Ni:** Resources, Methodology, Data curation, Conceptualization. **Wen-Xing Ding:** Writing – review & editing, Validation, Supervision, Funding acquisition, Formal analysis, Conceptualization.

Data availability statement

The data supporting this study's findings are available from the corresponding author upon reasonable request.

Declaration of competing interest

Wen-Xing Ding is an associate editor for *Liver Research* and was not involved in the editorial review or the decision to publish this article. The authors declare that they have no known competing financial interests or personal relationships that could have appeared to influence the work reported in this paper.

Acknowledgements

This study was partly supported by the National Institutes of Health funds R37 AA020518, R21 AA030617, and R01AA031230 (WXD). Sha Neisha Williams was supported by NIH/NIAAA F31AA031623. Migrated *vs.* resident hepatic macrophages isolated from the mouse models were provided by the Cell Bank Repository of the NIAAA-supported Integrative Liver Cell Core (R24AA012885) of the University of Southern California.

References

1. Narro GEC, Díaz LA, Ortega EK, et al. Alcohol-related liver disease: a global perspective. *Ann Hepatol.* 2024;29:101499. https://doi.org/10.1016/j.aohep.2024.8101499.

2. Mackowiak B, Fu Y, Maccioni L, Gao B. Alcohol-associated liver disease. *J Clin Invest*. 2024;134:e176345. https://doi.org/10.1172/JCI176345.
3. Ma X, Chen A, Melo L, et al. Loss of hepatic DRP1 exacerbates alcoholic hepatitis by inducing megamitochondria and mitochondrial maladaptation. *Hepatology*. 2023;77:159–175. https://doi.org/10.1002/hep.32604.
4. Chao X, Wang S, Ma X, et al. Persistent mTORC1 activation due to loss of liver Tuberous sclerosis complex 1 promotes liver injury in alcoholic hepatitis. *Hepatology*. 2023;78:503–517. https://doi.org/10.1097/HEP.0000000000000373.
5. Huang DQ, Mathurin P, Cortez-Pinto H, Loomba R. Global epidemiology of alcohol-associated cirrhosis and HCC: trends, projections and risk factors. *Nat Rev Gastroenterol Hepatol*. 2023;20:37–49. https://doi.org/10.1038/s41575-022-00688-6.
6. Williams JA, Manley S, Ding WX. New advances in molecular mechanisms and emerging therapeutic targets in alcoholic liver diseases. *World J Gastroenterol*. 2014;20:12908–12933. https://doi.org/10.3748/wjg.v20.i36.12908.
7. Feng D, Hwang S, Guillot A, et al. Inflammation in alcohol-associated hepatitis: pathogenesis and therapeutic targets. *Cell Mol Gastroenterol Hepatol*. 2024;18:101352. https://doi.org/10.1016/j.jcmgh.2024.04.009.
8. Slevin E, Baiocchi L, Wu N, et al. Kupffer cells: inflammation pathways and cell-cell interactions in alcohol-associated liver disease. *Am J Pathol*. 2020;190:2185–2193. https://doi.org/10.1016/j.ajpath.2020.08.014.
9. Fox ES, Thomas P, Broitman SA. Comparative studies of endotoxin uptake by isolated rat Kupffer and peritoneal cells. *Infect Immun*. 1987;55:2962–2966. https://doi.org/10.1128/iai.55.12.2962-2966.1987.
10. Nguyen-Lefebvre AT, Horuzsko A. Kupffer cell metabolism and function. *J Enzymol Metabol*. 2015;1:101.
11. Uesugi T, Froh M, Arteel GE, Bradford BU, Thurman RG. Toll-like receptor 4 is involved in the mechanism of early alcohol-induced liver injury in mice. *Hepatology*. 2001;34:101–108. https://doi.org/10.1053/jhep.2001.25350.
12. Osna NA, Donohue Jr TM, Kharbanda KK. Alcoholic liver disease: pathogenesis and current management. *Alcohol Res*. 2017;38:147–161.
13. Ceni E, Mello T, Galli A. Pathogenesis of alcoholic liver disease: role of oxidative metabolism. *World J Gastroenterol*. 2014;20:17756–17772. https://doi.org/10.3748/wjg.v20.i47.17756.
14. Park BJ, Lee YJ, Lee HR. Chronic liver inflammation: clinical implications beyond alcoholic liver disease. *World J Gastroenterol*. 2014;20:2168–2175. https://doi.org/10.3748/wjg.v20.i9.2168.
15. Nagy LE. Recent insights into the role of the innate immune system in the development of alcoholic liver disease. *Exp Biol Med (Maywood)*. 2003;228:882–890. https://doi.org/10.1177/153537020322800803.
16. Gao B, Bataller R. Alcoholic liver disease: pathogenesis and new therapeutic targets. *Gastroenterology*. 2011;141:1572–1585. https://doi.org/10.1053/j.gastro.2011.09.002.
17. Padmanaban S, Baek JW, Chamarthy SS, et al. Nanoparticle-based therapeutic strategies for chronic liver diseases: advances and insights. *Liver Res*. 2025;9:104–117. https://doi.org/10.1016/j.livres.2025.04.002.
18. Glick D, Barth S, Macleod KF. Autophagy: cellular and molecular mechanisms. *J Pathol*. 2010;221:3–12. https://doi.org/10.1002/path.2697.
19. Deter RL, De Duve C. Influence of glucagon, an inducer of cellular autophagy, on some physical properties of rat liver lysosomes. *J Cell Biol*. 1967;33:437–449. https://doi.org/10.1083/jcb.33.2.437.
20. Klionsky DJ, Emr SD. Autophagy as a regulated pathway of cellular degradation. *Science*. 2000;290:1717–1721. https://doi.org/10.1126/science.290.5497.1717.
21. Yu L, Chen Y, Tooze SA. Autophagy pathway: cellular and molecular mechanisms. *Autophagy*. 2018;14:207–215. https://doi.org/10.1080/15548627.2017.1378838.
22. Qian H, Chao X, Williams J, et al. Autophagy in liver diseases: a review. *Mol Aspects Med*. 2021:100973. https://doi.org/10.1016/j.mam.2021.100973.
23. Yan S. Role of TFEB in autophagy and the pathogenesis of liver diseases. *Biomolecules*. 2022;12:672. https://doi.org/10.3390/biom12050672.
24. Napolitano G, Ballabio A. TFEB at a glance. *J Cell Sci*. 2016;129:2475–2481. https://doi.org/10.1242/jcs.146365.
25. Franco-Juarez B, Coronel-Cruz C, Hernandez-Ochoa B, et al. TFEB; beyond its role as an autophagy and lysosomes regulator. *Cells*. 2022;11:3153. https://doi.org/10.3390/cells11193153.
26. Settembre C, Di Malta C, Polito VA, et al. TFEB links autophagy to lysosomal biogenesis. *Science*. 2011;332:1429–1433. https://doi.org/10.1126/science.1204592.
27. Yang CB, Liu J, Tong BC, et al. TFEB, a master regulator of autophagy and biogenesis, unexpectedly promotes apoptosis in response to the cyclopentenone prostaglandin 15d-PGJ2. *Acta Pharmacol Sin*. 2022;43:1251–1263. https://doi.org/10.1038/s41401-021-00711-7.
28. Tan A, Prasad R, Jho EH. TFEB regulates pluripotency transcriptional network in mouse embryonic stem cells independent of autophagy-lysosomal biogenesis. *Cell Death Dis*. 2021;12:343. https://doi.org/10.1038/s41419-021-03632-9.
29. Javaheri A, Bajpai G, Picataggi A, et al. TFEB activation in macrophages attenuates postmyocardial infarction ventricular dysfunction independently of ATG5-mediated autophagy. *JCI Insight*. 2019;4:e127312. https://doi.org/10.1172/jci.insight.127312.
30. Mortimore GE, Hutson NJ, Surmacz CA. Quantitative correlation between proteolysis and macro- and microautophagy in mouse hepatocytes during starvation and refeeding. *Proc Natl Acad Sci U S A*. 1983;80:2179–2183. https://doi.org/10.1073/pnas.80.8.2179.
31. Chao X, Ni HM, Ding WX. Insufficient autophagy: a novel autophagic flux scenario uncovered by impaired liver TFEB-mediated lysosomal biogenesis from chronic alcohol-drinking mice. *Autophagy*. 2018;14:1646–1648. https://doi.org/10.1080/15548627.2018.1489170.
32. Ding WX, Li M, Chen X, et al. Autophagy reduces acute ethanol-induced hepatotoxicity and steatosis in mice. *Gastroenterology*. 2010;139:1740–1752. https://doi.org/10.1053/j.gastro.2010.07.041.
33. Chao X, Wang S, Zhao K, et al. Impaired TFEB-mediated lysosome biogenesis and autophagy promote chronic ethanol-induced liver injury and steatosis in mice. *Gastroenterology*. 2018;155:865–879 (e12). https://doi.org/10.1053/j.gastro.2018.05.027.
34. Williams JA, Ni HM, Ding Y, Ding WX. Parkin regulates mitophagy and mitochondrial function to protect against alcohol-induced liver injury and steatosis in mice. *Am J Physiol Gastrointest Liver Physiol*. 2015;309:G324–G340. https://doi.org/10.1152/ajpgi.00108.2015.
35. Bertola A, Mathews S, Ki SH, Wang H, Gao B. Mouse model of chronic and binge ethanol feeding (the NIAAA model). *Nat Protoc*. 2013;8:627–637. https://doi.org/10.1038/nprot.2013.032.
36. Smedsrod B, Pertoft H. Preparation of pure hepatocytes and reticuloendothelial cells in high yield from a single rat liver by means of Percoll centrifugation and selective adherence. *J Leukoc Biol*. 1985;38:213–230. https://doi.org/10.1002/jlb.38.2.213.
37. Ni HM, McGill MR, Chao X, et al. Removal of acetaminophen protein adducts by autophagy protects against acetaminophen-induced liver injury in mice. *J Hepatol*. 2016;65:354–362. https://doi.org/10.1016/j.jhep.2016.04.025.
38. Xu J, Chi F, Guo T, et al. NOTCH reprograms mitochondrial metabolism for proinflammatory macrophage activation. *J Clin Investig*. 2015;125:1579–1590. https://doi.org/10.1172/JCI76468.
39. Qian H, Chao X, Wang S, et al. Loss of SQSTM1/p62 induces obesity and exacerbates alcohol-induced liver injury in aged mice. *Cell Mol Gastroenterol Hepatol*. 2023;15:1027–1049. https://doi.org/10.1016/j.jcmgh.2023.01.016.
40. Guan Y, Peiffer B, Feng D, et al. IL-8+ neutrophils drive inexorable inflammation in severe alcohol-associated hepatitis. *J Clin Invest*. 2024;134:e178616. https://doi.org/10.1172/JCI178616.
41. Martina JA, Chen Y, Gucek M, Puertollano R. MTORC1 functions as a transcriptional regulator of autophagy by preventing nuclear transport of TFEB. *Autophagy*. 2012;8:903–914. https://doi.org/10.4161/auto.19653.
42. Medzhitov R, Horng T. Transcriptional control of the inflammatory response. *Nat Rev Immunol*. 2009;9:692–703. https://doi.org/10.1038/nri2634.
43. Colbert JD, Matthews SP, Miller G, Watts C. Diverse regulatory roles for lysosomal proteases in the immune response. *Eur J Immunol*. 2009;39:2955–2965. https://doi.org/10.1002/eji.200939650.
44. JJo EK, Yuk JM, Shin DM, Sasakawa C. Roles of autophagy in elimination of intracellular bacterial pathogens. *Front Immunol*. 2013;4:97. https://doi.org/10.3389/fimmu.2013.00097.
45. Pastore N, Brady OA, Diab HI, et al. TFEB and TFE3 cooperate in the regulation of the innate immune response in activated macrophages. *Autophagy*. 2016;12:1240–1258. https://doi.org/10.1080/15548627.2016.1179405.
46. Ilyas G, Cingolani F, Zhao E, Tanaka K, Czaja MJ. Decreased macrophage autophagy promotes liver injury and inflammation from alcohol. *Alcohol Clin Exp Res*. 2019;43:1403–1413. https://doi.org/10.1111/acer.14041.
47. Settembre C, Medina DL. TFEB and the CLEAR network. *Methods Cell Biol*. 2015;126:45–62. https://doi.org/10.1016/bs.mcb.2014.11.011.
48. Wang S, Ni HM, Chao X, et al. Critical role of TFEB-mediated lysosomal biogenesis in alcohol-induced pancreatitis in mice and humans. *Cell Mol Gastroenterol Hepatol*. 2020;10:59–81. https://doi.org/10.1016/j.jcmgh.2020.01.008.
49. Wang S, Ni HM, Chao X, et al. Impaired TFEB-mediated lysosomal biogenesis promotes the development of pancreatitis in mice and is associated with human pancreatitis. *Autophagy*. 2019;15:1954–1969. https://doi.org/10.1080/15548627.2019.1596486.
50. Li Z, Zhao J, Zhang S, Weinman SA. FOXO3-dependent apoptosis limits alcohol-induced liver inflammation by promoting infiltrating macrophage differentiation. *Cell Death Discov*. 2018;4:16. https://doi.org/10.1038/s41420-017-0020-7.
51. Cohen JI, Chen X, Nagy LE. Redox signaling and the innate immune system in alcoholic liver disease. *Antioxid Redox Signal*. 2011;15:523–534. https://doi.org/10.1089/ars.2010.3746.
52. Kim HH, Shim YR, Choi SE, et al. Catecholamine induces Kupffer cell apoptosis via growth differentiation factor 15 in alcohol-associated liver disease. *Exp Mol Med*. 2023;55:158–170. https://doi.org/10.1038/s12276-022-00921-x.
53. Wang Y, Guan Y, Feng D, et al. Infiltrating macrophages replace Kupffer cells and play diverse roles in severe alcohol-associated hepatitis. *Cell Mol Immunol*. 2025;22:1262–1275. https://doi.org/10.1038/s41423-025-01343-1.
54. Wang M, You Q, Lor K, Chen F, Gao B, Ju C. Chronic alcohol ingestion modulates hepatic macrophage populations and functions in mice. *J Leukoc Biol*. 2014;96:657–665. https://doi.org/10.1189/jlb.6A0114-004RR.
55. Guan Y, Feng D, Maccioni L, Wang Y, Gao B. New therapeutic target for alcohol-associated hepatitis (AH): AH-associated IL-8(+) neutrophils. *eGastroenterology*. 2024;2:e100166. https://doi.org/10.1136/egastro-2024-100166.